Rev.Adv.Mater.Sci. 11 (2006) 46-55

DISLOCATION EMISSION FROM NANOVOIDS IN SINGLE-PHASE AND COMPOSITE NANOCRYSTALLINE MATERIALS*

I.A. Ovid'ko and A.G. Sheinerman

Institute of Problems of Mechanical Engineering, Russian Academy of Sciences, Bolshoj 61, Vasil. Ostrov, St. Petersburg 199178, Russia

Received: December 10, 2005

Abstract. A theoretical model is suggested which describes the role of nanoscale voids (nanovoids) as sources of dislocations in single-phase and composite nanocrystalline materials during plastic deformation. In the framework of the model, lattice and grain boundary (GB) dislocations are emitted from nanovoids under the shear stress action. The characteristic values of the flow stress needed to initiate dislocation emission from nanovoids are estimated and shown to be close to those that characterize plastic flow in nanocrystalline materials. With the results of the suggested theoretical model, the effects of nanovoids on deformation and fracture processes in single-phase and composite nanocrystalline materials are discussed.

* Presented at the 2nd International Conference "Nanomaterials and Nanotechnologies" (Crete, Greece, June 14-18, 2005)

1. INTRODUCTION

The unique mechanical properties of single-phase and composite nanocrystalline materials (nanomaterials) represent the subject of intensive research; see, e.g. [1–20]. These properties are caused by interface and nanoscale effects associated with the structural peculiarities of nanomaterials. In particular, high-density ensembles of interfaces (grain and interphase boundaries) in nanomaterials effectively hamper the slip of lattice dislocations, basic carriers of plastic flow in conventional coarse-grained polycrystals. As a corollary, the values of yield stress for nanomaterials are commonly 2–10 times larger than those for their coarse-grained counterparts; see reviews [1–6] and references therein. In nanomaterials with finest grains (whose grain size L is lower than a critical value L_c lying in the range from 10 to 30 nm), lattice dislocation slip is almost completely suppressed, and GBs carry plastic flow by such deformation mechanisms as intergrain sliding, Coble creep mode and rotational deformation mode; see book [20] and reviews [1–6]. Besides, deformation twins nucleated at GBs contribute to plastic flow [7,8,10–12,21]. These plastic deformation mechanisms operate in nanomaterials with finest grains at very high values of the applied stress. In nanomaterials with intermediate grains (whose grain size L lies in the range $L_c<L<100$ nm), lattice dislocations are still the main carriers of

Corresponding author: I.A. Ovid'ko, e-mail: ovidko@def.ipme.ru

plastic flow, as with coarse-grained polycrystals. However, the action of Frank-Read sources of lattice dislocations is hampered in intermediate grains of deformed nanomaterials, in which case alternative dislocation sources should come into play. Following experimental data [7,8,10–12,21–23], computer simulations [24–26] and theoretical models [16,27–30], lattice dislocations are effectively emitted by GBs and their triple junctions in nanomaterials during plastic deformation. In 'in-situ' experiments [23] and molecular dynamics simulations [31], emission of lattice dislocations from tips of rapidly growing cracks in mechanically loaded nanomaterials has been observed. Besides rapidly growing cracks, nanovoids – carriers of slow ductile fracture – often exist in deformed nanomaterials [1,23]. In many cases, nanovoids are nucleated in nanomaterials during their fabrication. Also, nanovoids can be intensively nucleated at local stress concentrators in nanomaterials during plastic deformation [1,23,32–34]. Since nanovoids are typical elements of the defect structure of nanomaterials under mechanical load, it is very important to understand their role in the unusual deformation behavior of nanomaterials. We think that nanovoids can serve as lattice dislocation sources alternative to conventional Frank-Read sources, brittle crack tips, GBs and their triple junctions, and thus strongly affect plastic flow characteristics of nanomaterials. This view is indirectly supported by the experimental data and results of theoretical analysis [35] indicating the void growth by lattice dislocation emission in monocrystalline copper under laser shock load at which ultrahigh mechanical stresses operate. Since ultrahigh mechanical stresses commonly exist in nanomaterials under quasi-static deformation, it is natural to think that nanovoids – typical structural elements of nanomaterials – can emit dislocations in these materials. The main aim of this paper is to suggest a theoretical model which describes the nanovoids as sources of lattice and interfacial dislocations in single-phase and composite nanocrystalline materials during plastic deformation.

2. NANOVOIDS AS SOURCES OF INDIVIDUAL LATTICE AND INTERFACIAL DISLOCATIONS IN DEFORMED NANOMATERIALS

In this section, we theoretically examine the energy characteristics of emission of individual dislocations by nanovoids in deformed nanomaterials. Following [14,32], the nucleation of nanovoids and nanocracks occurs at GBs and is driven by a dramatic release of stresses of either several dislocations with elemental Burgers vectors or individual superdislocations with large Burgers vector (Fig. 1). In this case, nanovoids absorb the (super)dislocations and thereby serve as stress sources characterized by large Burgers vectors [32]. This is a specific feature of nanovoids in nanomaterials, differentiating them from dislocation-free voids theoretically considered by Lubarda *et al.* [35] in the case of monocrystalline copper.

For the analysis of the energy characteristics of emission of individual dislocations by nanovoids nucleated at GBs in deformed nanomaterials, we consider a model dislocated nanovoid in a plastically deformed solid subjected to the action of an external shear stress $\tau = -\tau_{xy}$ (Fig. 2). Such a nanovoid can serve as a dislocation source due to dislocation reactions whose typical examples are presented in Fig. 2. For simplicity of mathematics, the nanovoid is assumed to have a cylindrical form (Fig. 2). Let the nanovoid have a radius R_0 and contain an edge superdislocation with a Burgers vector $\boldsymbol{B}$ (hereinafter called the *B*-superdislocation) (Fig. 2a). Let the *B*-superdislocation split into an immobile superdislocation with a Burgers vector $\boldsymbol{b}_1$ (hereinafter called the b_1-superdislocation) and a mobile dislocation with a Burgers vector $\boldsymbol{b}_2$, located in either GB (Fig. 2b) or grain interior (Fig. 2c). The mobile dislocation (hereinafter called the b_2-dislocation) moves along the *x*-axis over a distance *d* from the nanovoid center (Figs. 2b and 2c). The Burgers vectors of the superdislocations and the mobile dislocations are supposed to be oriented parallel to the *x*-axis (Figs. 2a, 2b, and 2c), that is, $\boldsymbol{B} = B_x \boldsymbol{e}_x$, $\boldsymbol{b}_1 = b_{1x} \boldsymbol{e}_x$, $\boldsymbol{b}_2 = b_{2x} \boldsymbol{e}_x$. They obey the conservation law during the splitting transformation: $B = \boldsymbol{b}_1 + \boldsymbol{b}_2$.

In order to reveal the necessary conditions for the splitting transformation shown in Figs. 2a, 2b, and 2c, we find the energy difference ΔW_{sp} related to this transformation. The energy difference ΔW_{sp} consists of six terms:

$$\Delta W_{sp} = W_{b_1} + W_{b_2} - W_B + W_{b_1 - b_2} + W_c - A_\tau . \qquad (1)$$

Here W_{b1}, W_{b2}, and W_B are the proper energies of the b_1-superdislocation, the mobile b_2-dislocation, and the *B*-superdislocation, respectively. $W_{b1\text{-}b2}$ denotes the energy of the elastic interaction between the b_1-superdislocation and b_2-dislocation, W_c is the energy of the b_2-dislocation core, and A_τ is the work of the external shear stress τ, spent to transfer of

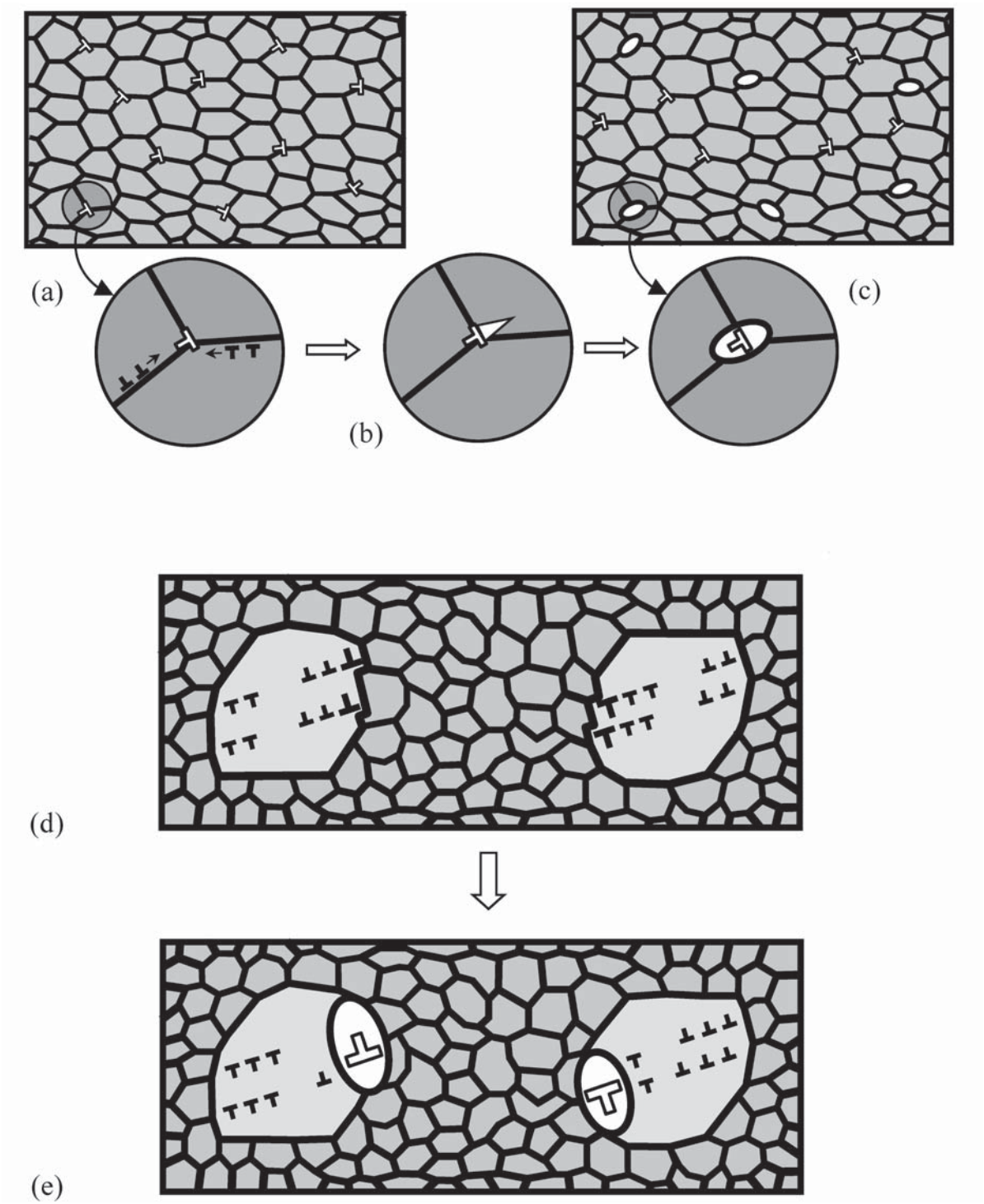

Fig. 1. Formation of nanovoids (serving as stress sources of superdislocation type) in deformed nanomaterials. (a) Nanocrystalline material is deformed by grain boundary sliding. The magnified inset in (a) highlights grain boundary dislocations (carriers of grain boundary sliding) that move along boundary planes and form a superdislocation at triple junction. (b) Large-scale view of nucleation of a flat nanocrack at triple junction due to release of stresses of triple junction superdislocation. (c) Elliptic nanovoids in nanocrystalline material result from transformations of flat nanocracks. The magnified inset in (c) highlights an elliptic nanovoid serving as stress source of the superdislocation type. (d) Plastic deformation of a nanocomposite consisting of a nanocrystalline matrix and large ductile inclusions of the second phase. Lattice dislocations glide in large inclusions towards interphase boundaries (separating the large inclusions and nanoscale grains in the nanocomposite) where they converge and form superdislocations at boundary steps. (e) Plastic deformation of a nanocomposite consisting of a nanocrystalline matrix and large ductile inclusions of the second phase. Nanovoids are nucleated at interphase boundaries due to release of stresses of superdislocations. The nanovoids contain superdislocations and thereby serve as stress sources of the superdislocation type.

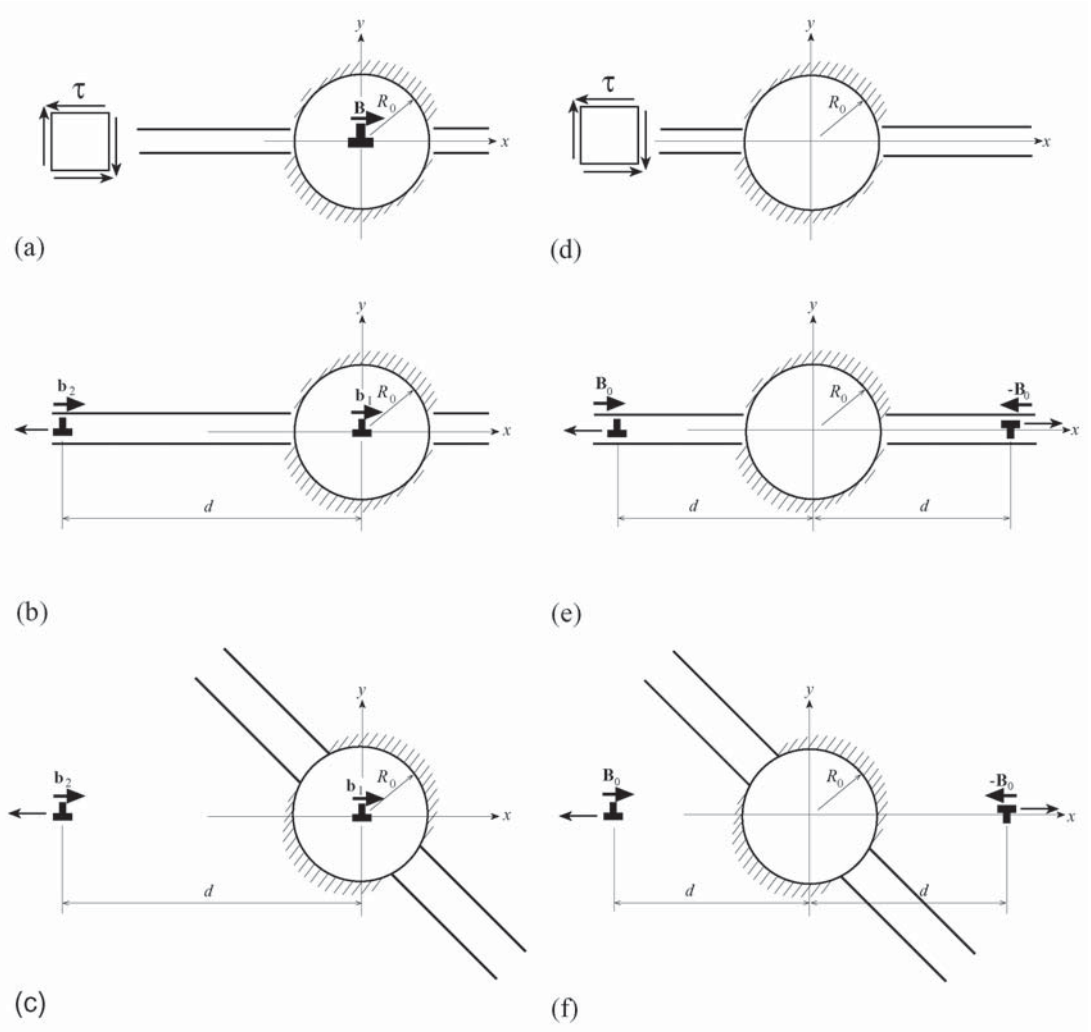

Fig. 2. Emission of lattice and grain boundary dislocations from cylindrical nanovoids. (a), (b) and (c) Splitting of edge dislocation in cylindrical nanovoid. (a) Dislocated cylindrical nanovoid. (b) Splitting of dislocation (with Burgers vector ***B***) in cylindrical nanovoid into dislocation with Burgers vector $\boldsymbol{b}_1$, located inside the nanovoid, and grain boundary dislocation with Burgers vector $\boldsymbol{b}_2$, which moves outside the nanovoid. (c) Splitting of dislocation (with Burgers vector ***B***) in cylindrical nanovoid into dislocation with Burgers vector $\boldsymbol{b}_1$, located inside the nanovoid, and lattice dislocation with Burgers vector $\boldsymbol{b}_2$, which moves outside the nanovoid. (d), (e),and (f) Emission of two edge dislocations from non-dislocated cylindrical nanovoid. (d) The initial state. (e) Two grain boundary dislocations with Burgers vectors $\boldsymbol{B}_0$ and - $\boldsymbol{B}_0$ are emitted from the nanovoid and move in opposite directions. (f) Two lattice dislocations with Burgers vectors $\boldsymbol{B}_0$ and - $\boldsymbol{B}_0$ are emitted from the nanovoid and move in opposite directions.

the b_2-dislocation from the nanovoid to its position distant by *d* from the cylindrical nanovoid center.

Generally speaking, dislocation emission from nanovoids is accompanied by ledge formation at the nanovoid internal surface. The ledge energy contributes to the energy balance characterizing the dislocation emission from the nanovoid. Lubarda *et al.* [35] assumed that the ledge energy increases the energy barrier for dislocation emission. However, the internal surface of any nanovoid is rough, in which case surface ledge formation related to dislocation emission can either increase or decrease the internal surface roughness. Moreover, dislocation emission is enhanced at those places of a rough

nanovoid at which ledge formation decreases the surface roughness. With uncertainty of the ledge energy contribution to the energy balance and its statistical character, we neglect this contribution in our further analysis.

The elastic energies figuring in formula (1) are calculated with the use of the stress function [36,37] for an edge dislocation in an elastically isotropic medium containing an infinite cylindrical pore. The work A_τ is calculated using the expressions [38] for the stress field in a solid (containing a cylindrical pore) under a remote uniform shear load. After some algebra (omitted here), we find the expression for the characteristic energy difference ΔW_{sp}. In the typical case of (R_0, d - R_0) >> r_0, where r_0 is the b_2-dislocation core cutoff radius, we have:

$$\Delta W_{sp} = \frac{Db_2^2}{2}\left\{\ln\frac{R_0}{r_0} + \ln\left(\tilde{d}^2 - 1\right)\right\} + \frac{Db_2^2}{2}\left\{1 - \frac{B_x}{b_{2x}}\left(2\ln\tilde{d} + \frac{1}{\tilde{d}^2}\right)\right\} - \frac{Db_2^2}{2}\left\{\frac{2\tau R_0}{Db_{2x}}\left(\tilde{d} - \frac{2}{\tilde{d}} + \frac{1}{\tilde{d}^3}\right)\right\}, \quad (2)$$

where $\tilde{d} = d/R_0$, $D = G/[2\pi(1-\nu)]$, G is the shear modulus, and ν Poisson's ratio.

The force F acting on the b_2-dislocation due to the effects of both the dislocated nanovoid and the external shear stress $\tau = -\tau_{xy}$ is calculated using formula (2) and the condition $F = -\partial\Delta W_{sp}/\partial d$. The force F defined in this way is positive if the dislocation $\boldsymbol{b}_2$ is repelled from the dislocated nanovoid and negative if it is attracted to this nanovoid. F is given as

$$F = -\frac{Db_2^2}{R_0}\left(\frac{\tilde{d}}{\tilde{d}^2-1} - \frac{B_x}{b_{2x}}\frac{\tilde{d}^2-1}{\tilde{d}^3}\right) + \frac{Db_2^2}{R_0}\left(\frac{\tau R_0}{Db_{2x}}\frac{\left(\tilde{d}^2-1\right)\left(\tilde{d}^2+3\right)}{\tilde{d}^4}\right). \quad (3)$$

In the limit of $R_0 \to \infty$ for $\tau = 0$ and a finite specified distance $H = d - R_0$ between the b_2-dislocation and the nanovoid free surface, formula (3) is reduced to the image force $F^i = -Db_2^2/(2H)$ acting on an edge dislocation distant by H from a flat free surface. In the case of $\tau = 0$ and a large distance $d >> R_0$ between the b_2-dislocation and the nanovoid center, the force F is tentatively equal to the force of the interaction between the b_1- and b_2-dislocations in an infinite medium: $F(d >> R_0, \tau = 0) = Db_1b_2/d$.

The dependences of F on d/R_0 are presented in Fig. 3a, for various values of the parameters b_{2x}/B_x and $\tau R_0/(Db_{2x})$. In the situation where the external shear stress is absent ($\tau = 0$), the dependences in question are shown as dashed curves in Fig. 3a. In this situation, the force F acting on the b_2-dislocation is the sum of the image force exerted by the nanovoid free surface and the force exerted by the b_1-dislocation. If $b_{2x}/B_x = 1$, we have: $b_1 = 0$, and the

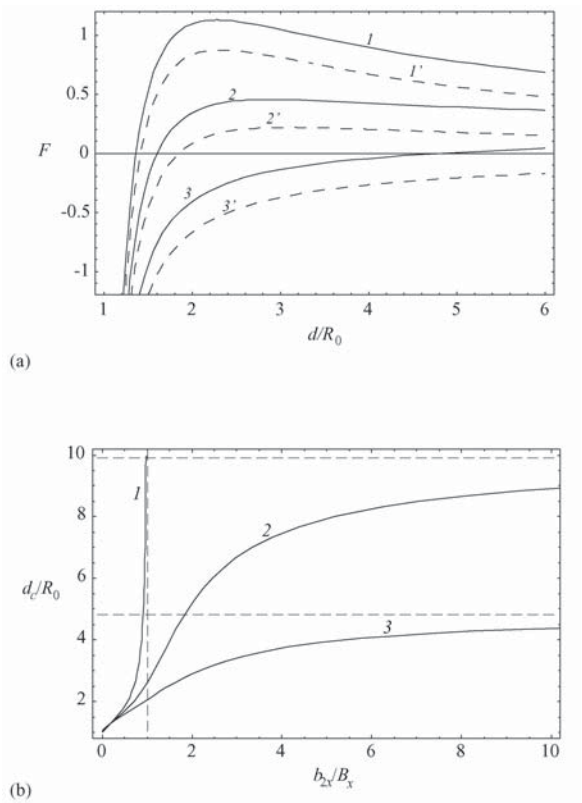

Fig. 3. Characteristic dependences for splitting of edge dislocation in a cylindrical nanovoid. (a) Dependences of the force F (in units of Db_2^2/R_0) acting on b_2-dislocation on non-dimensional distance d/R_0 between this dislocation and nanovoid center, for $\tau R_0/(Db_{2x}) = 0.2$ (solid curves 1,2,and 3), and $\tau = 0$ (dashed curves 1', 2',and 3'); $b_{2x}/B_x = 0.25$ (curves 1 and 1'), 0.5 (curves 2 and 2'), and ∞ (curves 3 and 3'). (b) Dependences of non-dimensional critical distance d_c/R_0 on ratio b_{2x}/B_x, for $\tau R_0/(Db_{2x}) = 0$, 0.1 and 0.2 (curves 1, 2 and 3, respectively). Horizontal and vertical lines show asymptotes to curves.

interaction between the b_2-dislocation and the nanovoid is short-range ($|F|$ falls as d^{-3} with rising d). For $b_{2x}/B_x \neq 1$, we have: $b_1 \neq 0$, and the interaction between the b_2-dislocation and the dislocated nanovoid is long-range ($|F|$ falls as d^{-1} at large d). When $0 < b_{2x}/B_x < 1$, the Burgers vectors $\boldsymbol{b}_1$ and $\boldsymbol{b}_2$ have the same direction, and the b_2-dislocation has an unstable equilibrium position $d = d_c$ near the nanovoid; d_c is derived from the condition $F(d= d_c) = 0$ (see curves 1' and 2' in Fig. 3a). In contrast, in the cases $b_{2x}/B_x \geq 1$ or $b_{2x}/B_x < 0$ in which the b_1- and b_2-dislocations have opposite directions of the Burgers vectors, the b_2-dislocation is attracted to the nanovoid at any distance H from it (see curve 3' in Fig. 3a).

Thus, emitting of a dislocation by the void with a superdislocation requires overcoming an energetic barrier. Therefore, the opportunity for superdislocation split depends on the possibility of overcoming this energetic barrier in the course of plastic deformation. If $\Delta W_{sp}(d = R_0 + b_2) < 0$, which is the case if a superdislocation in the nanovoid splits out a much smaller dislocation, the magnitude W_b of the energetic barrier may be calculated as: $W_b = \Delta W_{sp}(d = d_c) - \Delta W_{sp}(d= R_0 + b_2)$. In this case, W_b is equal to the difference of the system energies in the state where the split dislocation is located at the critical distance d_c from the nanovoid center and the state where this dislocation is located at the minimum possible distance b_2 from the nanovoid surface. In contrast, if $\Delta W_{sp}(d=R_0+b_2) > 0$, we have: $W_b = W_{sp}(d = d_c)$.

In a first approximation, the probability P of dislocation split in a given time t may be estimated from the Arrhenius-law-like formula

$$\frac{dP}{dt} = \upsilon_D \exp\left[-\frac{bW_b}{k_B T}\right](1-P), \qquad (4)$$

where $v_D \approx 10^{13} s^{-1}$ is the Debye frequency, k_B the Boltzmann constant and T the absolute temperature. The product of the first two factors on the right hand side of formula (4) gives the average number of split acts per unit time, while the third factor 1-P expresses the probability that split has not yet occurred at the time t. With the relation $P(t=0)=0$, the solution to Eq. (4) has the form

$$P = 1 - \exp\left[-\upsilon_D t\, e^{-bW_b/(k_B T)}\right]. \qquad (5)$$

For the characteristic values $b_{2x} = b$ (where b is the magnitude of the lattice dislocation Burgers vector), $B_x = 4b$, $\tau/D = 0.02$, and $R_0/b_2 = 10$, one obtains: $d_c/R_0 \approx 1.37$. Substitution of these values of d_c and formula (2) to the definition of W_b yields: $W_b \approx 0.37Db_2^2$. In the case of Ni at the room temperature, we have: G = 73 GPa, ν = 0.34, b = 0.250 nm and T = 300 K. Then, even for the small time t = 0.02 s, we obtain: $P \approx 0.99$. For Cu, we have: G = 44 GPa, ν = 0.38, b = 0.256 nm. For Al: G = 27 GPa, ν = 0.31, b = 0.286 nm. For Cu and Al, we obtain that P = 0.99 for $t = 10^{-5}$ s and $t = 2 \cdot 10^{-7}$ s, respectively. This implies that for the case of Ni, Cu and Al the energetic barrier for dislocation split in a nanovoid may be easily overcome.

Now consider the partial case where an originally dislocation-free nanovoid emits a lattice dislocation. In this case, we obtain: $B_x = 0$. Then, for characteristic parameter values $\tau/D = 0.02$ and $R_0/b_2 = 10$, we have: $d_c/R_0 \approx 4.84$, which yields: $W_b = 2.26Db^2_2$. In this case, for Cu at the room temperature, one obtains that the probability P of lattice dislocation emission is negligibly small even at very large times t. The same result also applies to Al and Ni. That is, emission of a lattice dislocation from an originally dislocation-free nanovoid is not realistic at the room temperature. (Lattice dislocation emission from an originally dislocation-free nanovoid was also considered by Lubarda *et al.* [35]. They found that dislocation emission can occur in monocrystalline copper at high temperatures.) In contrast, in the situation where an originally dislocation-free nanovoid emits a GB dislocation with a three times smaller Burgers vector to an adjacent GB, we obtain that $P \approx 1$ even at negligibly small values of time t. Therefore, emission of a GB dislocation from an originally dislocation-free nanovoid is probable at the room temperature.

3. NANOVOIDS AS SOURCES OF DISLOCATION DIPOLES IN DEFORMED NANOMATERIALS

Let us consider the situation where the cylindrical nanovoid in its initial state does not contain dislocations and then emits two edge dislocations with opposite Burgers vectors $\boldsymbol{B}_0$ and $-\boldsymbol{B}_0$ (Figs. 2d, 2e, and 2f). The emitted dislocations glide in opposite directions as shown in Figs. 2e and 2f, for GB and lattice dislocations, respectively. In order to estimate the conditions at which the above emission of a dipole of edge dislocations from the dislocation-free cylindrical nanovoid is energetically favorable, we calculate the corresponding energy difference $\Delta\widetilde{W}$. This energy is calculated in the same way as the energy difference ΔW_{sp}. In doing so, we find the final expression for $\Delta\widetilde{W}$ to be as follows:

$$\Delta\tilde{W} = DB_0^2\left[\ln\frac{2d}{r_0} + \ln\frac{\tilde{d}^2-1}{\tilde{d}^2+1}\right] + DB_0^2\left[1-\frac{1}{\tilde{d}^2}-\frac{\tilde{d}^4-2\tilde{d}^2-1}{\tilde{d}^2\left(\tilde{d}^2+1\right)^2}\right] - DB_0^2\left[\frac{2\tau R_0}{DB_0}\left(\tilde{d}-\frac{2}{\tilde{d}}+\frac{1}{\tilde{d}^3}\right)\right], \quad (6)$$

where d is the distance between the dislocations and the nanovoid central line and $\tilde{d}=d/R_0$, as above.

The force $\tilde{F}$ acting on the edge dislocations is derived from the definition $\tilde{F}=-(1/2)\partial\Delta\tilde{W}/\partial d$ and formula (6) as follows:

$$\tilde{F} = \frac{DB_0^2}{2R_0}\left[-\frac{\tilde{d}^8+10\tilde{d}^6+6\tilde{d}^2-1}{\tilde{d}\left(\tilde{d}^2+1\right)^3\left(\tilde{d}^2-1\right)}\right] + \frac{DB_0^2}{2R_0}\left[\frac{2\tau R_0}{DB_0}\frac{\left(\tilde{d}^2-1\right)\left(\tilde{d}^2+3\right)}{\tilde{d}^4}\right]. \quad (7)$$

When the force $\tilde{F}$ is positive (negative, respectively), the dislocations are repelled from (attracted to, respectively) the cylindrical nanovoid. The dependences $\tilde{F}(d/R_0)$, calculated with formula (7), are presented in Fig. 4, for various values of the parameter $\tau R_0/(DB_0)$. As follows from Fig. 4, there is an unstable equilibrium position $d=\tilde{d}_c$ for the dislocations near the cylindrical nanovoid; it is derived from the condition $\tilde{F}(d=d_c)=0$. When $d<\tilde{d}_c$, the dislocations are attracted to the nanovoid. When $d>\tilde{d}_c$, the dislocations are repelled from the nanovoid. The value of $\tilde{d}_c$ decreases with rising the external shear stress τ.

Let us compare curve 1 in Fig. 4 and curve 3 in Fig. 3a, characterizing the emission of a dislocation dipole (Figs. 2d, 2e, and 2f) and the emission of one dislocation, respectively, from the non-dislocated cylindrical nanovoid. The comparison shows that, for the same values of the external stress τ and the Burgers vector magnitudes of the emitted dislocations ($B_0 = b_2$), we have: $\tilde{d}_c < d_c$. Thus, the nanovoid attraction region, which the dislocations have to pass through, is smaller for a dislocation dipole emitted from a non-dislocated nanovoid (Figs. 2d, 2e, and 2f), compared to that for one dislocation emitted from such a nanovoid. Moreover, the calculations demonstrate that the energetic barrier in the case of emission of a dislocation dipole is smaller than that in the case of emission of a single dislocation. The calculations also show that in the case of Cu, Al and Ni at the room temperature, a dipole of GB dislocations emitting from an originally dislocation-free nanovoid may easily overcome this energetic barrier. However, this energetic barrier proves to be too high for such a nanovoid to emit a dipole of lattice dislocations.

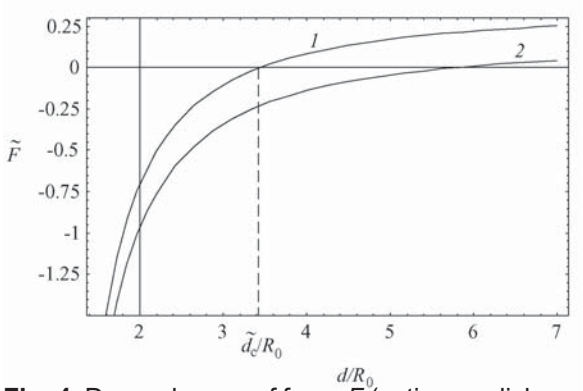

Fig. 4. Dependences of force $\tilde{F}$ (acting on dislocation with Burgers vector B_0) on nondimensional distance d/R_0 between the dislocation line and cylindrical nanovoid central line, for $\tau R_0/(DB_0) = 0.2$ and 0.1 (curves 1 and 2, respectively). The force F is given in units of $DB^2_0/(2R_0)$.

4. CONCLUDING REMARKS

Thus, following the results of our theoretical analysis, nanovoids can play the role of sources of both lattice and interfacial dislocations in deformed nanomaterials. The emission of a dislocation by a nanovoid is characterized by an energy barrier related to the elastic attraction between the emitted dislocation and the nanovoid. If the dislocation moves over a critical distance d_c from the nanovoid, the repulsion force comes into play which tends to move the dislocation far from the nanovoid. The values of the critical distance d_c and the energy barrier are sensitive to both the shear stress acting on the dislocation and geometric characteristics of the dislocation and the nanovoid. In particular, the energy barrier decreases with decreasing the dislocation Burgers vector magnitude and/or rising the shear stress. As a corollary, nanovoids very effectively emit GB dislocations with small Burgers vector magnitudes in nanomaterials commonly deformed at high mechanical stresses and characterized by large volume fractions of the GB phase. In these circum-

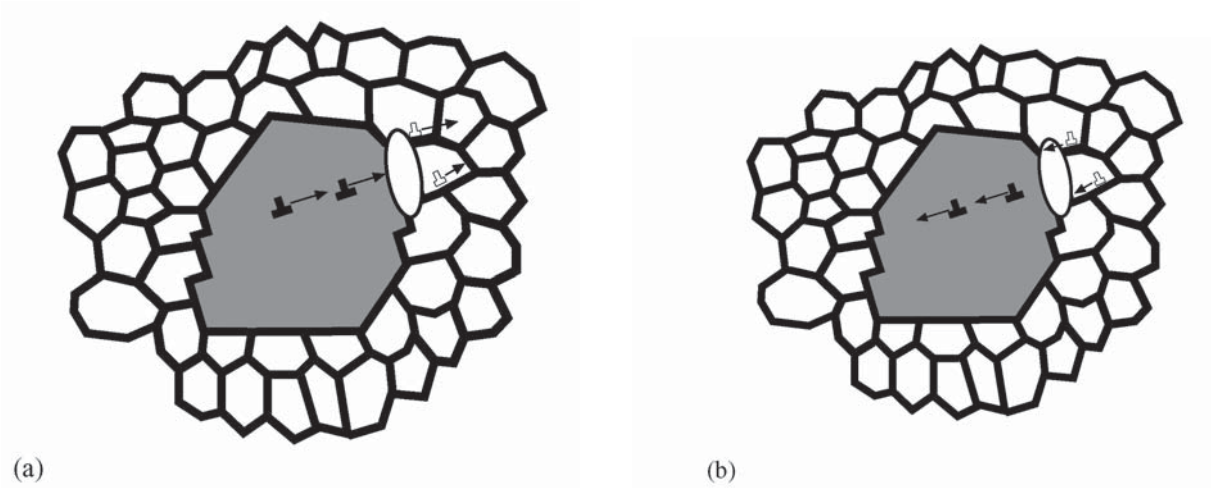

Fig. 5. Transformations of deformation mechanisms at nanovoid nucleating at grain boundary dividing nanocrystalline matrix and large grain in bimodal structure. (a) Lattice dislocation slip transforms into intergrain sliding. Moving lattice dislocations that carry lattice slip in large grain move towards nanovoid where they transform into gliding grain boundary dislocations that carry intergrain sliding in nanocrystalline matrix. (b) Intergrain sliding transforms into lattice dislocation slip. Gliding grain boundary dislocations that carry intergrain sliding in nanocrystalline matrix move towards nanovoid where they transform into moving lattice dislocations that carry lattice slip in large grain.

stances, as with voids growing by lattice dislocation emission in shock-loaded monocrystalline copper [35], nanovoids in deformed nanomaterials can effectively grow by emission of GB dislocations. This statement is of crucial importance for understanding the mechanism by which nanovoids grow and coalesce causing the experimentally observed [1,13,33,34,39,40] ductile dimples at fracture surfaces of deformed nanomaterials. A detailed theoretical analysis of nanovoid growth and coalescence by dislocation emission in nanomaterials will be the subject of our further investigations.

Besides fracture processes, plastic flow in nanomaterials can also be influenced by dislocation emission from nanovoids. For instance, with the role of nanovoids as sources of both lattice and GB dislocations, they can serve as structural defects providing effective transfer of plastic flow between neighboring structural units, that is, transfer of plastic flow from a grain to a neighboring grain, from a grain to an adjacent GB, from a GB to an adjacent GB, and from a GB to an adjacent grain. In particular, this role of nanovoids is important in transformations from one deformation mode to another in deformed nanomaterials. For instance, lattice dislocation slip in grains can effectively transform through stable nanovoids into intergrain sliding in neighboring GBs and vice versa.

Such transformations between different deformation mechanisms are of particular importance in single-phase nanomaterials with a bimodal structure consisting of a strong nanocrystalline matrix with ductile large grains [41–44] and nanocomposites consisting of a strong nanocrystalline matrix with ductile large inclusions of the second phase [45,46]. In the cases under consideration, different deformation mechanisms dominate in different structural elements of nanocomposites and bimodal nanomaterials. Lattice dislocation slip is dominant in both large ductile inclusions in nanocomposites and large ductile grains in bimodal nanomaterials [41–46]. At the same time, the nanocrystalline matrix with finest grains is intensively deformed through deformation mechanisms conducted by interfaces, in particular, through intergrain sliding [3,4,20]. In these circumstances, plastic flow is highly inhomogeneous at interfaces dividing the nanocrystalline matrix and large ductile inclusions/grains. The nanovoids at such interfaces can provide effective transformations from one deformation mechanism to another mechanism, thus smoothing plastic deformation in nanocomposites and bimodal nanomaterials. For instance, lattice dislocation slip in large inclusions/grains can effectively transform through nanovoids into intergrain sliding along neighboring GBs in the nanocrystalline

matrix (Fig. 5a) and vice versa (Fig. 5b). The discussed transformations between different plastic deformation mechanisms operating in different neighboring structural elements of nanocomposites and bimodal nanomaterials can contribute to the experimentally detected [41–46] substantial ductility of these materials.

ACKNOWLEDGEMENTS

This work was supported, in part, by the Offce of US Naval Research (grant N00014-05-1-0217), INTAS (grant 03-51-3779), INTAS-AIRBUS (grant 04-80-7339), Russian Academy of Sciences Program 'Structural Mechanics of Materials and Construction Elements', and St. Petersburg Scientific Center.

REFERENCES

[1] K.S. Kumar, S. Suresh and H. Swygenhoven // *Acta Mater*. **51** (2003) 5743.
[2] X. Zhang, H. Wang and C.C. Koch // *Rev. Adv. Mater. Sci*. **6** (2004) 53.
[3] B.Q. Han, E. Lavernia and F.A. Mohamed // *Rev. Adv. Mater. Sci*. **9** (2005) 1.
[4] I.A. Ovid'ko // *Int. Mater. Sci.* **50** (2005) 65.
[5] I.A. Ovid'ko // *Rev. Adv. Mater. Sci*. **10** (2005) 89.
[6] G.-D. Zhan and A.K. Mukherjee // *Rev. Adv. Mater. Sci*. **10** (2005) 185.
[7] X.Z. Liao, F. Zhou, E.J. Lavernia, S.G. Srinivasan, M.I. Baskes, D.W. He and Y.T. Zhu // *Appl. Phys. Lett*. **83** (2003) 632.
[8] X.Z. Liao, F. Zhou, E.J. Lavernia, D.W. He and Y.T. Zhu // *Appl. Phys. Lett*. **83** (2003) 5062.
[9] S.V. Bobylev, M.Yu. Gutkin and I.A. Ovid'ko // *J. Phys. D* **37** (2004) 269.
[10] Y.T. Zhu, X.R. Liao, S.G. Srivansan, Y.H. Zhao, M.I. Baskes, F. Zhou and E.J. Lavernia // *Appl. Phys. Lett.* **85** (2004) 549.
[11] X.Z. Liao, Y.H. Zhao, S.G. Srinivasan, Y.T. Zhu, R.Z. Valiev and D.V. Gunderov // *Appl. Phys. Lett.* **84** (2004) 592.
[12] X.Z. Liao, S.G. Srinivasan, Y.H. Zhao, M.I. Baskes, Y.T. Zhu, F. Zhou, E.J. Lavernia and H.F. Xu // *Appl. Phys. Lett.* **84** (2004) 3564.
[13] H. Li and F. Ebrahimi // *Appl. Phys. Lett.* **84** (2004) 4307.
[14] I.A. Ovid'ko and A.G. Sheinerman // *Acta Mater*. **52** (2004) 1201; *Acta Mater*. **53** (2005) 1347.
[15] K.M. Youssef, R.O. Scattergood, K.L. Murty, J.A. Horton and C.C. Koch // *Appl. Phys. Lett.* **87** (2005) 091904.
[16] M.Yu. Gutkin, I.A. Ovid'ko and N.V. Skiba // *J. Phys. D* **38** (2005) 3921.
[17] M.Yu. Gutkin and I.A. Ovid'ko // *Appl. Phys. Lett*. **87** (2005) 251916.
[18] Y.T. Zhu, X.R. Liao and R.Z. Valiev // *Appl. Phys. Lett*. **86** (2005) 103112.
[19] Y.M. Wang, A.M. Hodge, J. Biener, A.V. Hamza, D.E. Barnes, K. Liu and T.G. Nieh // *Appl. Phys. Lett*. **86** (2005) 101915.
[20] M.Yu. Gutkin and I.A. Ovid'ko, *Plastic Deformation in Nanocrystalline Materials* (Springer, Berlin-Heidelberg-New York, 2004).
[21] M. Chen, E. Ma, K.J. Hemker, H. Sheng, Y. Wang and X. Cheng // *Science* **300** (2003) 1275.
[22] A.K. Mukherjee // *Mater. Sci. Eng. A* **322** (2002) 1.
[23] K.S. Kumar, S. Suresh, M.F. Chisholm, J.A. Horton and P. Wang // *Acta Mater*. (2003) **51** 387.
[24] H. van Swygenhoven, M. Spaczer, A. Caro and D. Farkas // *Phys. Rev. B* **60** (1999) 22.
[25] H. van Swygenhoven and P.M. Derlet // *Phys. Rev. B* **64** (2001) 224105.
[26] J. Schiotz // *Scr. Mater*. **51** (2004) 837.
[27] M.Yu. Gutkin, A.L. Kolesnikova, I.A. Ovid'ko and N.V. Skiba // *Phil. Mag. Lett*. **81** (2002) 651.
[28] R.J. Asaro, P. Krysl and B. Kad // *Phil. Mag. Lett.* **83** (2003) 733.
[29] S.V. Bobylev, M.Yu. Gutkin and I.A. Ovid'ko // *Acta Mater*. **52** (2004) 3793; *Phys. Rev. B*, in press.
[30] R.J. Asaro and S. Suresh // *Acta Mater*. **53** (2005) 3369.
[31] D. Farkas, H. van Swygenhoven and P.M. Derlet // *Phys. Rev. B* **66** (2002) 060101.
[32] I.A. Ovid'ko and A.G. Sheinerman // *Phil. Mag.* **86** (2006), in press.
[33] H. Li and F. Ebrahimi // *Adv. Mater*. **17** (2005) 1969.
[34] R.C. Hugo, H. Kung, J.R. Weertman, R. Mitra, J.A. Knapp, D.M. Follstaedt // *Acta Mater.* **51** (2003) 1937.
[35] V.A. Lubarda, M.S. Schneider, D.H. Kalantar, B.A. Remington and M.A. Meyers // *Acta Mater.* **52** (2004) 1397.
[36] J. Dundurs, In: *Recent Advances in Engineering Science, Vol. 2*, ed. by A.C. Eringen (Gordon & Breach, New York, 1967) p. 223.

[37] T. Mura, In: *Advances in Materials Research, Vol. 3*, ed. by H. Herman (Interscience Publ., New York, 1968) p. 1.
[38] S.P. Timoshenko and J. Goodier, *Theory of Elasticity* (McGraw-Hill, New York, 1970).
[39] K.M. Youssef, R.O. Scattergood, K.L. Murty and C.C. Koch // *Appl. Phys. Lett.* **85** (2004) 929.
[40] K.M. Youssef, R.O. Scattergood, K.L. Murty and C.C. Koch // *Scr. Mater.* **54** (2006) 251.
[41] V.L. Tellkamp, A. Melmed and E.J. Lavernia // *Metall. Mater. Trans. A* **32** (2001) 2335.
[42] Y. Wang, M. Chen, F. Zhou and E. Ma // *Nature* **419** (2002) 912.
[43] A.V. Sergueeva, N.A. Mara and A.K. Mukherjee // *Rev. Adv. Mater. Sci*. **7** (2004) 67.
[44] Y.M. Wang and E. Ma // *Acta Mater*. **52** (2004) 1699.
[45] G. He, J. Eckert, W. Loeser and L. Schultz // *Nature Mat.* **2** (2003) 33.
[46] G. He, M. Hagiwara, J. Eckert and W. Loeser // *Phil. Mag. Lett*. **84** (2004) 365.